Desalination and Water Treatment
www.deswater.com

doi: 10.1080/19443994.2016.1157763

57 (2016) 26063–26072
November

Taylor & Francis
Taylor & Francis Group

Impact of key geochemical parameters on the attenuation of Pb(II) from water using a novel magnetic nanocomposite: fulvic acid-coated magnetite nanoparticles

Qingchun Fu[a], Baowei Hu[b,*], Xiaode Zhou[a], Qingyuan Hu[b], Jiang Sheng[c,*]

[a]*Institute of Water Resources and Hydro-electric Engineering, Xi'an University of Technology, Xi'an 710048, P.R. China, emails: fuqingch@126.com (Q. Fu), zhouxd1962@126.com (X. Zhou)*
[b]*Key Laboratory of Clean Dyeing and Finishing Technology of Zhejiang Province, School of Life Science, College of Yuanpei, Shaoxing University, Huancheng West Road 508, Shaoxing 312000, P.R. China, Tel./Fax: +86 575 88341820; emails: hbw@usx.edu.cn (B. Hu), QinyuanHu32@126.com (Q. Hu)*
[c]*Ningbo Institute of Materials Technology & Engineering, Chinese Academy of Sciences, Ningbo 315201, P.R. China, email: shengjiang@nimte.ac.cn*

Received 6 October 2015; Accepted 18 February 2016

ABSTRACT

In recent years, magnetic nanoparticles have been widely utilized as promising adsorbents for fast and effective attenuation of metal ions in water in environmental pollution control. Herein, a novel magnetic nanocomposite, namely fulvic acid (FA)-coated Fe_3O_4 nanoparticles (Fe_3O_4/FA), was utilized for the attenuation of Pb(II) in water by an adsorption process. The results indicated that the coated FA reduced the surface oxidation and agglomeration of Fe_3O_4 particles and thus promoted the performance of Fe_3O_4/FA towards Pb(II) removal. The results indicate that Pb(II) adsorption on Fe_3O_4/FA obtained equilibrium in less than 2 h. Besides, the adsorption of Pb(II) on Fe_3O_4/FA is strongly dependent on medium pH, and independent of ionic strength and the type of coexisted ions. So, inner-sphere surface complexation mainly controls Pb(II) uptake on Fe_3O_4/FA. The Fe_3O_4/FA also showed good regeneration property and separation convenience for the treatment of Pb(II). Besides, XPS is used to study the mechanism at a molecular level and to identify the species of Pb(II) on Fe_3O_4/FA. Results of this study showed that the magnetic Fe_3O_4/FA is a promising sequestrator for the attenuation and separation of heavy metal ions in water in environmental pollution cleanup.

Keywords: Fulvic acid; Magnetite; Coated; Attenuation; Geochemical parameters

1. Introduction

Water pollution by heavy metal ions and/or radionuclides, which are hazardous and non-biodegradable, has increasingly become a widespread problem, and has aroused worldwide concern of scientists and environmentalists. Recently, the levels of toxic heavy metal ions and/or radionuclides in the natural surface and ground waters have been greatly increased due to the pollution resulted from industrial and agricultural wastewater discharge [1–18]. Among these metal ions, lead (Pb(II)),

*Corresponding authors.

which is commonly used in many industrial processes such as printing, explosive manufacturing, pigments, and photographic materials, has been widely regarded to be detrimental to many human and living things [19–23]. For the sake of protecting public health and ecosystem stability, it is very necessary to treat Pb(II) and related metal ions before discharge into the environment in order to eliminate the potential dangerous to human beings and environment.

Thus far, a lot of methods have been utilized for the effective remediation of Pb(II) and related metal ions in water, which included chemical oxidation or reduction, ion exchange, membrane filtration, precipitation, and adsorption [19], among which adsorption technique has been regarded as a promising process for the natural attenuation of metal ions from subsurface water and wastewater. So, different kinds of novel adsorbents with high adsorption capacities and efficiencies such as clay minerals and modified carbon nanotubes have been under extensive investigations of many researchers [10–12,19–23]. As one of the most important potential adsorbents, magnetic nanomaterials such as magnetite (Fe_3O_4) are very much suitable for the sequestration of metal ions in water, since magnetite can be conveniently re-collected from water [24–29]. Nevertheless, the bare Fe_3O_4 can be very easily oxidized and aggregated in water, limiting the practical application of Fe_3O_4 in environmental remediation [25]. Concerning this issue, coating Fe_3O_4 with some organic substances such as cyclodextrin or humic acid (HA) could well decrease the oxidation and agglomeration of bare Fe_3O_4. Besides, the coating process could also enhance the adsorption of metal ions due to the strong complexation interaction of metal ions with the O-containing functional groups in these organic substances [25–28]. In our previous paper, we have coated fulvic acid (FA) onto Fe_3O_4 to obtain a Fe_3O_4/FA composite and found that Fe_3O_4/FA showed high adsorption to Ni(II) in water [29].

So, in order to extend the real application of the Fe_3O_4/FA composite in heavy metal remediation, herein, we investigated the applicability of Fe_3O_4/FA in the attenuation of Pb(II) in water with respect to rate and capacity via an adsorption process. The impact of key geochemical parameters including medium pH, ionic strength, solid content, and coexisted cationic or anionic ions on the adsorption of Pb(II) on the Fe_3O_4/FA was studied. The regeneration and reuse of Fe_3O_4/FA in Pb(II) attenuation was also investigated.

2. Experimental section

2.1. Materials and chemicals

All the chemicals used in our experiments were purchased in analytical purity. Analytical-grade lead nitrate was used to prepare Pb(II) stock solution with concentration of 1,000 mg/L, which was further diluted with deionized water to the required concentrations during the adsorption process. The FA-coated Fe_3O_4 composite was prepared according to our previous paper [29]. Briefly, ~8.0 g of $FeSO_4{\cdot}7H_2O$ and ~10.0 g of $FeCl_3{\cdot}6H_2O$ were dissolved in ~200 mL of water and heated to ~90˚C, and then, two solutions, ~20 mL of ammonium hydroxide and ~1.0 g of FA dissolved in ~100 mL of water, were added. The mixture was stirred at ~90˚C for 30 min and then cooled. The black precipitate was collected by filtrating and washed. The obtained precipitate was Fe_3O_4/FA and ready for use. The bare Fe_3O_4 was prepared in a similar way except that no FA was added [29].

2.2. Adsorption procedures

According to previous papers [2,10,29], the adsorption experiments were carried out in the polyethylene tubes by using batch technique. The stock solutions of adsorbents and $NaNO_3$ were mixed and shaken for two days to get equilibrium; then, stock Pb(II) solution was added to get desired concentrations. The medium pH was adjusted with ~0.01 mol/L HNO_3 or NaOH. The samples were shaken for another two days and filtered by 0.45 μm membrane filters. The results of Pb (II) adsorption on the polyethylene tube indicated that little Pb(II) can be adsorbed, suggesting that Pb(II) adsorption on the tube can be negligible. The concentration of Pb(II) was analyzed by spectrophotometry at ~616 nm using Pb-CAP-III complex. All the experimental data were the average of duplicate determinations, and the relative errors were ~5%. For reversibility and regeneration study, typical treatment process was conducted by adding 500 mL of 0.01 mol/L $NaNO_3$ and 10 mg/L Pb(II) into a 1-L beaker containing 0.3, 0.5, or 0.9 g/L Fe_3O_4 or Fe_3O_4/FA. The solution pH was adjusted to a certain value (~6.0). The suspensions were continuously stirred for 24 h using a mechanical mixer at room temperature, and then separated; the obtained supernatants were used for the measurement of Pb(II) concentration. The solid was washed with 0.001 mol/L HCl and high-purity Milli-Q water, until Pb(II) cannot be determined in the supernatants, collected and dried at 60˚C. The recovered Fe_3O_4 or Fe_3O_4/FA was used for the adsorption of Pb(II) in a second time. According to

this process, the adsorption–desorption process was repeated for 6 times.

2.3. Analytical methods

According to previous papers [22,24,29], the X-ray photoelectron spectroscopic (XPS) spectra were recorded with a thermo ESCALAB 250 spectrometer using an AlK*a* monochromator source and a multidetection analyzer under a 10^{-8} Pa residual pressure. Surface charging effects were corrected with C 1s peak at 284.6 eV as a reference. Thermo gravimetric analyzer and differential thermal analysis (TGA-DTA) measurements were carried out using a Shimadzu TGA-50 thermogravimetric analyzer from room temperature to 800°C at the heating rate of 10°C min^{-1} with a nitrogen flow rate of 100 mL min^{-1}. The surface morphology of the materials before and after adsorption was examined using field emission scanning electron microscope (SEM, JEOL JSM-6700F).

3. Results and discussion

3.1. Characterization

The surface elemental composition of the adsorbent materials can be determined by the XPS spectra. Fig. 1 shows the high-resolution O 1s spectra for the samples of Fe_3O_4 and Fe_3O_4/FA. The O 1s spectrum of Fe_3O_4 sample can be deconvoluted into O^{2-}, OH^-, and surface-adsorbed H_2O, while the O 1s spectrum of Fe_3O_4/FA sample can be deconvoluted into O–C=O (carboxyl group), C–O–C (ether group), and C–O (hydroxyl group), respectively. This result suggested the successful coating of FA on the Fe_3O_4 surface. The XPS spectra of Fe $2p_{3/2}$ at ~710 eV and Fe $2p_{1/2}$ at ~724 eV for the samples of Fe_3O_4 and Fe_3O_4/FA (Fig. 2) are indicative of the electron peaks of Fe 2p of Fe_2O_3 and Fe_3O_4. The peaks of $Fe2p_{3/2}$ and $Fe2p_{1/2}$ of the samples can be deconvoluted into two peaks of ~711.5 and ~724.7 eV for Fe_2O_3, and two peaks of ~710.2 and ~724.1 eV for Fe_3O_4, respectively [30]. The results indicated the surface oxidation of the adsorbent materials. Besides, peaking fitting results showed that the ratio of Fe_2O_3 to Fe_3O_4 for the Fe_3O_4/FA sample is lower that than for the Fe_3O_4 sample, revealing the good anti-oxidization performance of the Fe_3O_4/FA composite. The stability of the naked and FA-coated Fe_3O_4 particles are further investigated by thermogravimetric analysis, and the results are shown in Fig. 3. The weight loss occurs at 17–100°C due to the loss of physically adsorbed water on the particle surface. The weight loss of Fe_3O_4 at 100–250°C is higher than that of Fe_3O_4/FA, suggesting that Fe_3O_4/FA is more thermostable. The thermogravimetric analysis also confirms the successful coating of FA on the Fe_3O_4 surface [22]. The SEM images of the Fe_3O_4/FA particles before and after Pb(II) adsorption are shown in Fig. 4. It was clear that these particles display discrete spherical shape (Fig. 4(A)). After adsorption of Pb(II) ions, we can see that Pb(II) attached closely to Fe_3O_4/FA surface (Fig. 4(B)) due to the strong interaction of Pb(II) with the binding sites.

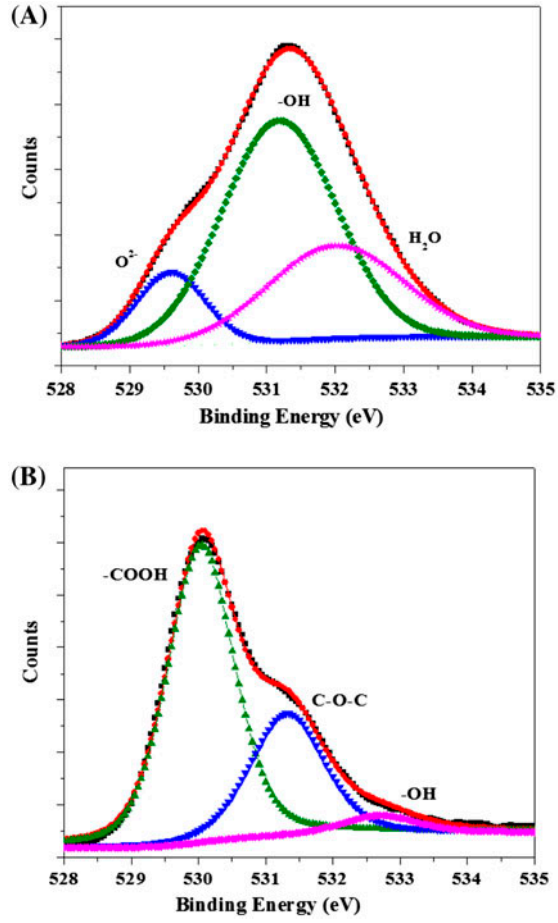

Fig. 1. XPS survey of O 1s spectra of (A) Fe_3O_4 and (B) Fe_3O_4/FA.

3.2. Impact of contact time

Fig. 5 shows the adsorption of Pb(II) on Fe_3O_4 and Fe_3O_4/FA as a function of contact time. One can see that adsorption of Pb(II) on both adsorbents increases rapidly at the initial contact time of 2 h, and then, Pb(II) adsorption maintains a high value with the increase in contact time. The whole adsorption consists of two distinct processes, i.e. an initial

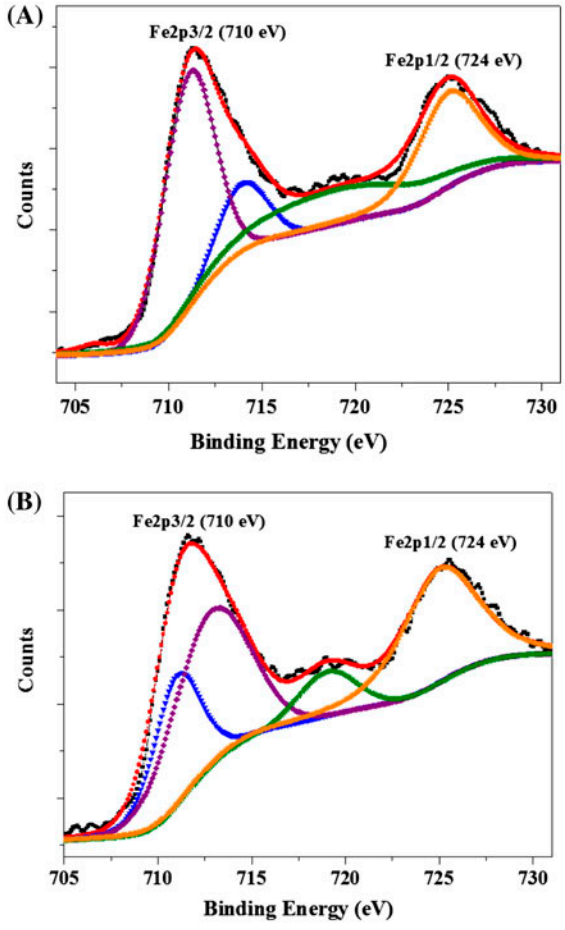

Fig. 2. XPS survey of Fe 2p spectra of (A) Fe_3O_4 and (B) Fe_3O_4/FA.

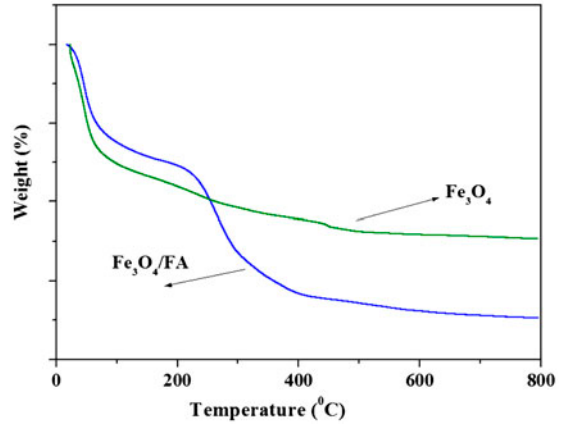

Fig. 3. TGA curves of Fe_3O_4 and Fe_3O_4/FA.

fast adsorption step, followed by a slow adsorption step. The fast Pb(II) adsorption is attributed to the rapid diffusion of Pb(II) from solution to the external surfaces of the adsorbents. The subsequent slow adsorption is attributed to the longer diffusion range of Pb(II) into the inner-sphere pores of the adsorbents [11,24]. Besides, we can see that Fe_3O_4/FA showed higher adsorption to Pb(II) than Fe_3O_4 did. The fast adsorption kinetics and high adsorption capacity of Fe_3O_4/FA indicated that it may have good potentialities for continuous water treatment systems.

3.3. Impact of adsorbent content

The adsorption of Pb(II) in water on Fe_3O_4/FA as a function of adsorbent content is shown in Fig. 6. We can see that Pb(II) adsorption increases with the increase in Fe_3O_4/FA content. With the increase in Fe_3O_4/FA content, the functional binding sites at Fe_3O_4/FA surfaces participating in Pb(II) adsorption increase, and thus, the removal of Pb(II) reasonably increases. It is well known that there are many O-containing functional groups present at the surface of Fe_3O_4/FA. These O-containing functional groups can provide binding sites to cooperate with Pb(II) ions on the surface of Fe_3O_4/FA. In addition, these hydrophilic groups also make Fe_3O_4/FA particles to be dispersed in water more easily [19]. The hydrophilic groups at the surface of Fe_3O_4/FA make Pb(II) ions to contact with Fe_3O_4/FA and to be adsorbed on Fe_3O_4/FA.

3.4. Impact of pH

In order to determine the impact of medium pH on the adsorption capacity of Fe_3O_4/FA, the adsorption system was conducted at different pH levels. Fig. 7 shows the results of the adsorption of Pb(II) on Fe_3O_4/FA by changing medium pH from 2.0 to 12.0. We can see that Pb(II) adsorption on Fe_3O_4/FA enhanced at pH 2.0–7.0, maintained the high level at pH 7.0–10.0, and then reduced at pH > 10.0. The medium pH after the adsorption of Pb(II) shifted a little to the acidic region, indicating that H^+ is released into water during the adsorption of Pb(II) on Fe_3O_4/FA [19–23]. The enhancement of Pb(II) adsorption on Fe_3O_4/FA with the increase in medium pH may be attributed to the surface properties of Fe_3O_4/FA with respect to the surface charge and dissociation of surface functional groups [19]. The surface of Fe_3O_4/FA contains a large number of functional groups and may become positively charged at low pH values due to the protonation reaction (i.e. $SOH + H^+ \Leftrightarrow SOH_2^+$). The electrostatic repulsion between Pb(II) ions and the positively charged binding site (SOH_2^+) on Fe_3O_4/FA

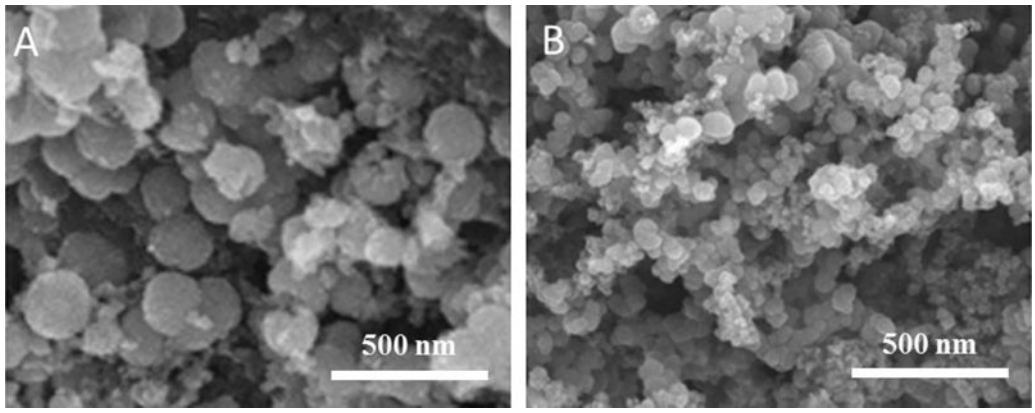

Fig. 4. SEM images of Fe_3O_4/FA before (A) and after (B) Pb(II) adsorption.

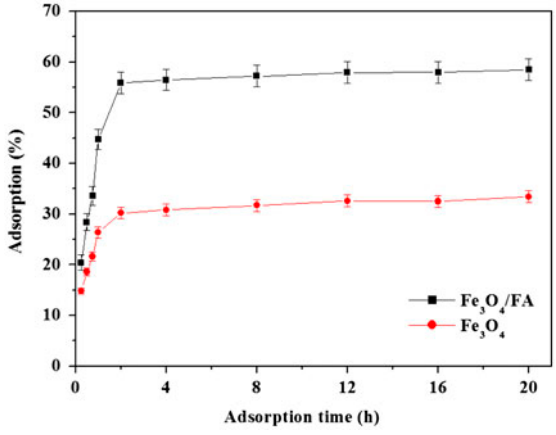

Fig. 5. Impact of contact time on the adsorption of Pb(II) on Fe_3O_4 and Fe_3O_4/FA pH 6.0, T = 293 K, the amount of material (Fe_3O_4 and Fe_3O_4/FA) was 0.5 g/L, the lead concentration of 10 mg/L.

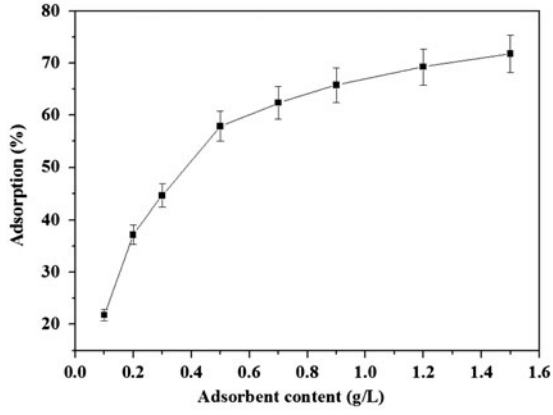

Fig. 6. Impact of solid content on the adsorption of Pb(II) on Fe_3O_4/FA, pH 6.0, T = 293 K, the lead concentration of 10 mg/L.

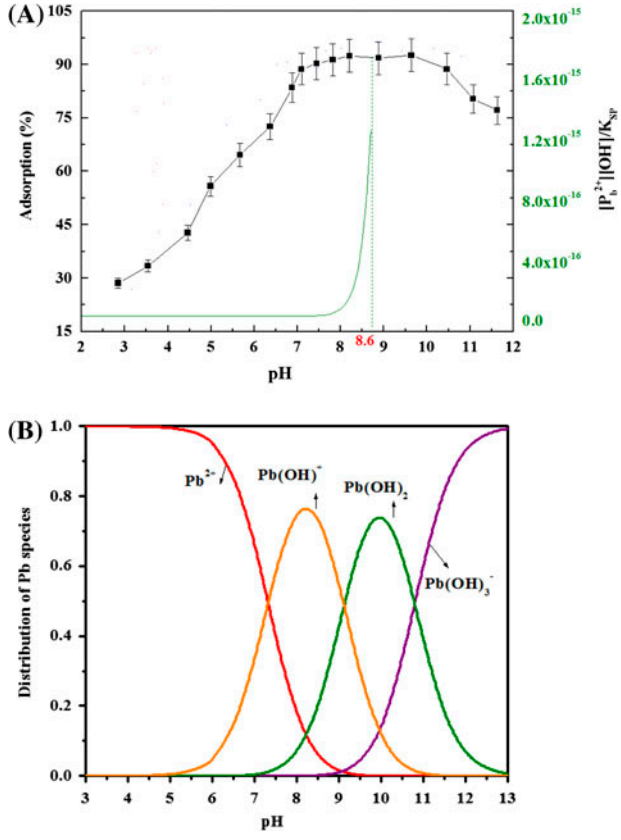

Fig. 7. (A) Impact of pH on the adsorption of Pb(II) on Fe_3O_4/FA, T = 293 K, the amount of material (Fe_3O_4 and Fe_3O_4/FA) was 0.5 g/L, the lead concentration of 10 mg/L and (B) distribution of Pb(II) species as a function of pH.

leads to the low adsorption. However, at high pH values, the surface of Fe_3O_4/FA becomes negatively charged due to the deprotonation reaction (i.e. $SOH \Leftrightarrow SO^- + H^+$) and electrostatic repulsion decreases, which enhances the adsorption of the

positively charged Pb(II) ions [19–23]. The exact species of Pb(II) impose a great impact on Pb(II) adsorption on Fe_3O_4/FA. Fig. 7(B) shows the relative distribution of Pb(II) species in water from their hydrolysis constants ($\log k_1 = 6.48$, $\log k_2 = 11.16$, $\log k_3 = 14.16$) [19]. It is clear that the species of Pb(II) are present in the forms of Pb^{2+}, $Pb(OH)^+$, $Pb(OH)_2^0$, and $Pb(OH)_3^-$ at different pH values. The main species is Pb^{2+} at pH < 7.0, and the removal of Pb^{2+} is controlled by an adsorption. At pH 7.0–10, the main species are $Pb(OH)^+$ and $Pb(OH)_2^0$ and they can be easily adsorbed on the negatively-charged surface of Fe_3O_4/FA. The main species are $Pb(OH)_2^0$ and $Pb(OH)_3^-$ at pH > 10.0; hence, the decrease in Pb(II) adsorption can be attributed to the competition reaction between OH^- and $Pb(OH)_3^-$. From the precipitation curve of Pb(II) in water (Fig. 7(A)), we can see that Pb(II) begins to form precipitation at pH 8.6. From these results, we can find that the best pH range of the adsorption system to attenuate Pb(II) in water using Fe_3O_4/FA is 7.0–10.0. The final pH values against the initial pH values are also determined. One can see (Table 1) that the final pH was lower than the initial pH with a value which decreased with the increase in the initial pH. The decrease in pH may be attributed to the release of H^+ from the surface of Fe_3O_4/FA into solution. With the increase in solution pH, the degree of deprotonation of Fe_3O_4/FA surface increased; thus, more Pb(II) ions were adsorbed and more H^+ ions were released into solution [29].

3.5. Impact of ionic strength

The ionic strength can impact the double electrode layer thickness and interface potential, hence, affecting the binding of the species of adsorbed ions. Generally regarding, outer-sphere surface complexation is dependent on ionic strength, while inner-sphere complexation is independent of ionic strength [31–38]. The impact of ionic strength on Pb(II) adsorption on Fe_3O_4 and Fe_3O_4/FA at pH 5.0 and 9.0 is shown in Fig. 8. We can see that Pb(II) adsorption on Fe_3O_4 is obviously affected by ionic strength at low pH values, and little impact on Pb(II) adsorption can be found at high pH values (Fig. 8(A)). So, we can conclude that outer-sphere surface complexation mainly contributes to Pb (II) adsorption on Fe_3O_4 at pH 5.0, while inner-sphere surface complexation is the main mechanism of Pb(II) adsorption on Fe_3O_4 at pH 9.0. However, the adsorption of Pb(II) on Fe_3O_4/FA was almost not impacted by ionic strength at both pH values (Fig. 8(B)), indicating that Pb(II) adsorption on Fe_3O_4/FA at both pH values is mainly controlled by inner-sphere surface complexation.

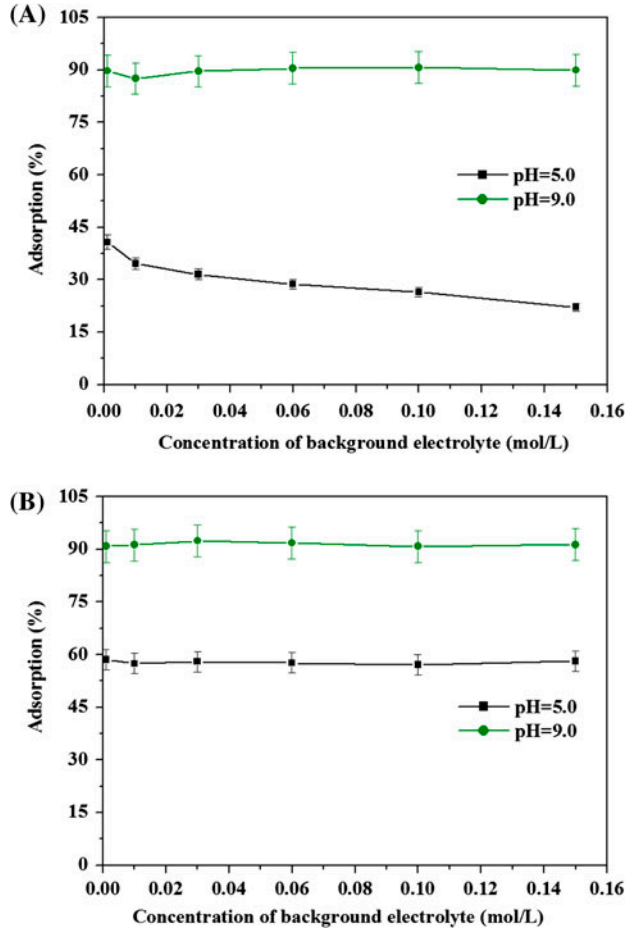

Fig. 8. Impact of concentration of background electrolyte on the adsorption of Pb(II) on (A) Fe_3O_4 and (B) Fe_3O_4/FA, T = 293 K, the amount of material (Fe_3O_4 and Fe_3O_4/FA) was 0.5 g/L, the lead concentration of 10 mg/L reaction for 24 h.

3.6. Regeneration and reuse

For the environmental sustainability of Fe_3O_4/FA, a high repeatability would add great value in the environmental pollution management [21,29]. In order

Table 1
The results of final pH values against the initial pH values

Initial pH	2.8	3.5	4.4	5.0	5.6	6.3	6.8	7.1	7.4	7.8	8.2	8.8
Final pH	1.7	2.6	3.4	3.9	4.7	5.1	5.4	5.5	5.8	6.2	7.0	7.3

to regenerate the adsorbents after adsorbing Pb(II), we used 0.1 mol/L HCl as a regeneration agent in this study. The adsorption of Pb(II) on Fe_3O_4 and Fe_3O_4/FA after 6 times of adsorption and desorption process at three different solid content was measured, and the results are shown in Fig. 9(A) and (B), respectively. The results suggested that the adsorption capacity and reusability of Fe_3O_4/FA are better than that of Fe_3O_4. The excellent repeatability of Fe_3O_4/FA indicated that the magnetic Fe_3O_4/FA composite is a promising candidate for the attenuation of metal ions in water. In previous studies, the adsorption of Pb(II) on lot of adsorbents such as Mg_2Al-layered double hydroxide [9], Na-bentonite [11], graphitic carbon nitride [13], graphene oxides [14], alginate gel beads [16], multi-walled carbon nanotubes and their modified composites [19,22,23], β-MnO_2 [20], and diatomite [21] have been extensively investigated. The results revealed that these adsorbents can be hardly re-collected from water when they are used for adsorption application. However, the Fe_3O_4/FA composite used herein is very much suitable for the sequestration of Pb(II) ions, because magnetite can be conveniently re-collected from water.

3.7. Impact of coexisted cationic or anionic ions

Fig. 10 shows the results of the impact of coexisted cationic or anionic ions on the adsorption of Pb(II) on Fe_3O_4/FA particles. We can see that Pb(II) adsorption on Fe_3O_4/FA is nearly not impacted by the coexisted cationic or anionic ions. Coexisted cationic ions in solution can compete for interaction with the binding sites of Fe_3O_4/FA, and Pb(II) have a higher affinity to

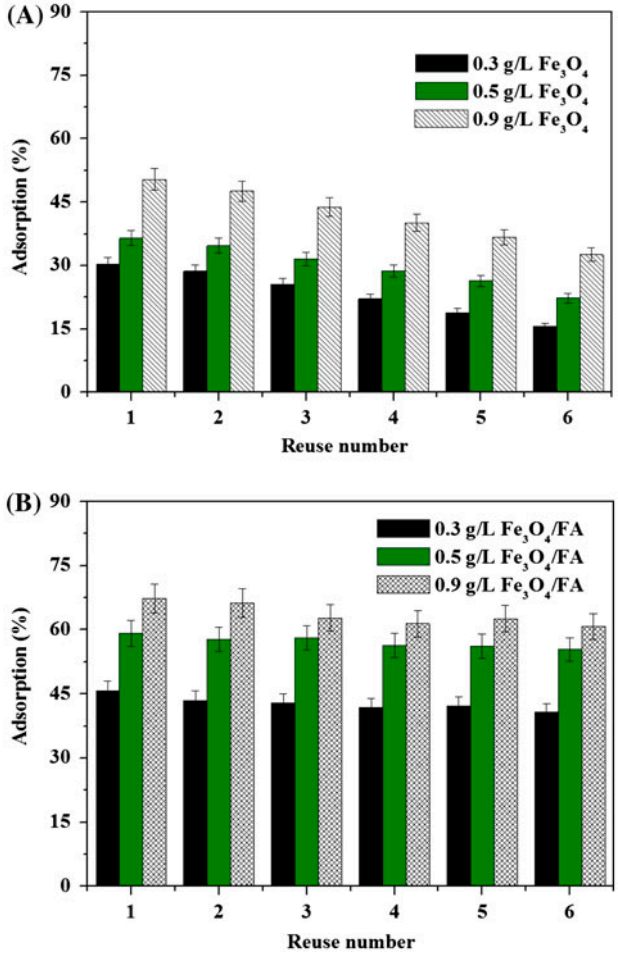

Fig. 9. The repeatability of (A) Fe_3O_4 and (B) Fe_3O_4/FA to Pb(II) via six times of adsorption and desorption process, the amounts of material were 2.3, 0.5, 0.9 g/L, respectively, pH 6.0, T = 293 K, the lead concentration of 10 mg/L.

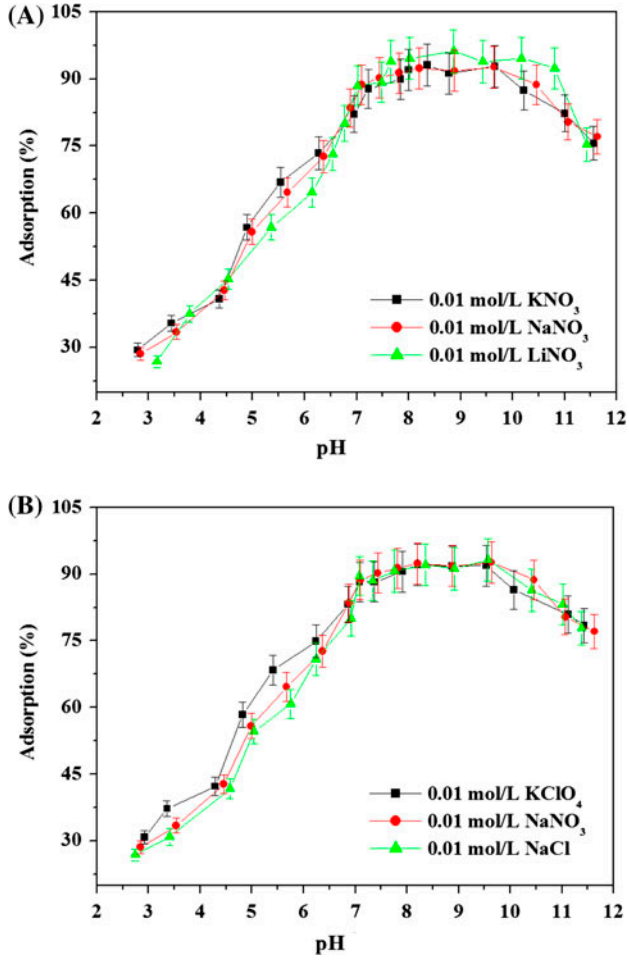

Fig. 10. Impact of coexisted (A) cationic or (B) anionic ions on the adsorption of Pb(II) on Fe_3O_4/FA T = 293 K, the amount of material (Fe_3O_4 and Fe_3O_4/FA) was 0.5 g/L, the lead concentration of 10 mg/L.

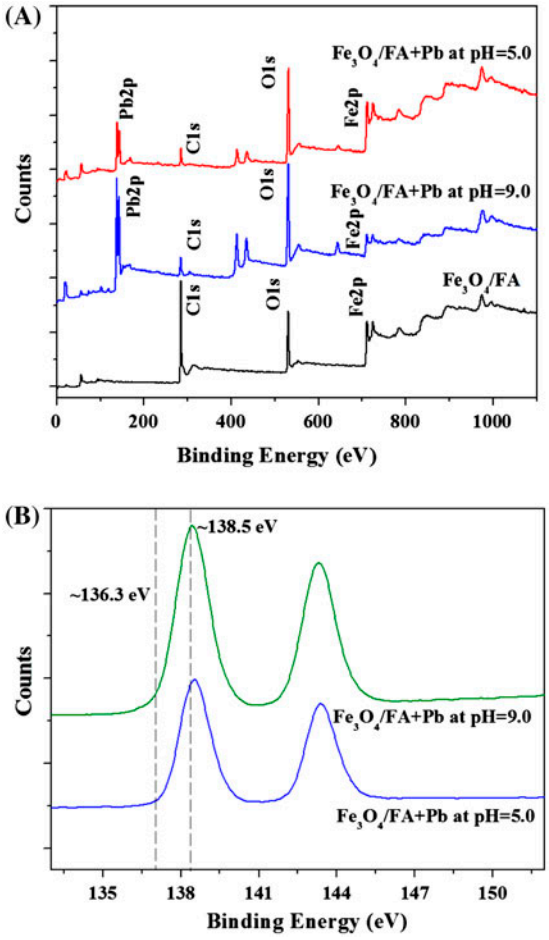

Fig. 11. (A) XPS wide survey of Fe_3O_4/FA before and after adsorption of Pb(II) and (B) XPS survey of Pb 4f spectra of the final solid sample.

the binding sites than the alkali metal ions; hence, the competition of alkali ions on Pb(II) adsorption Fe_3O_4/FA is almost negligible. The radicals radium order of the coexisted anionic ions is as follows: $Cl^- < NO_3^- < ClO_4^-$, the negatively charged anionic ions may form complexes with the functional groups on Fe_3O_4/FA surface [31–38]. Nevertheless, the impact of Cl^-, NO_3^-, and ClO_4^- on Pb(II) adsorption to Fe_3O_4/FA is still weak, suggesting the formation of surface complexes on Fe_3O_4/FA. So, the impact of coexisted anionic ions on Pb(II) adsorption from solution to Fe_3O_4/FA can also be negligible.

3.8. XPS investigation

In order to evaluate the variation in chemical information at Fe_3O_4/FA surface and the molecular level information of Pb(II) adsorption on Fe_3O_4/FA, a complementary description of the adsorption samples was obtained by XPS analysis. XPS techniques are carried out to identify the local atomic structures of Pb(II) adsorption on Fe_3O_4/FA. Typical XPS wide survey obtained for the samples of Fe_3O_4/FA before and after Pb(II) adsorption at pH 5.0 and pH 9.0 is shown in Fig. 11(A). An obvious peak appears at ~135 eV that is indicative of the presence of Pb for the adsorption sample, which is absent in the raw Fe_3O_4/FA before adsorption. Besides, the intensity of this peak for the adsorption sample at pH 9.0 is higher that than at pH 5.0; this is highly reasonable because of the higher adsorption of Pb(II) on Fe_3O_4/FA at pH 9.0. Fig. 11(B) displays the high-resolution Pb 4f spectra which shows two peaks including Pb $4f_{5/2}$ and Pb $4f_{7/2}$. The peak positions of Pb $4f_{5/2}$ and Pb $4f_{7/2}$ on Fe_3O_4/FA at pH 5.0 and pH 9.0 are quite similar, suggesting that Pb(II) adsorption to the same binding sites of Fe_3O_4/FA.

4. Conclusions

In conclusion, from the results of Pb(II) adsorption on Fe_3O_4/FA under the experimental conditions herein, we can obtain the following findings: The adsorption of Pb(II) on Fe_3O_4/FA achieves equilibrium rapidly. Adsorption of Pb(II) on Fe_3O_4/FA is strongly dependent on pH values but independent of ionic strength and coexisted cationic or anionic ions. Chemical interaction rather than physical interaction is the main mechanism responsible for the adsorption of Pb (II) on Fe_3O_4/FA. This material shows a great potential for the disposal of Pb(II)-contaminated wastewaters. According to the results for Pb(II), Fe_3O_4/FA may also be suitable for the attenuation of other heavy metal ions in water.

Acknowledgments

Financial supports from department of Science and Technology, Zhejiang province (2010C33101), financial supports from the National Natural Science Foundation of China (90610030) are acknowledged.

References

[1] S. Yang, G. Sheng, X. Tan, J. Hu, J. Du, G. Montavon, X. Wang, Determination of Ni(II) uptake mechanisms on mordenite surfaces: A combined macroscopic and microscopic approach, Geochim. Cosmochim. Acta 75 (2011) 6520–6534.
[2] G. Sheng, S. Yang, Y. Li, X. Gao, Y. Huang, X. Wang, Retention mechanisms and microstructure of Eu(III) on manganese dioxide studied by batch and high resolution EXAFS technique, Radiochim. Acta 102 (2014) 155–167.

[3] G. Sheng, Q. Yang, F. Peng, H. Li, X. Gao, Y. Huang, Determination of colloidal pyrolusite, Eu(III) and humic substance interaction: A combined batch and EXAFS approach, Chem. Eng. J. 245 (2014) 10–16.
[4] Q.H. Fan, X.L. Tan, J.X. Li, X.K. Wang, W.S. Wu, G. Montavon, Sorption of Eu(III) on attapulgite studied by batch, XPS, and EXAFS techniques, Environ. Sci. Technol. 43 (2009) 5776–5782.
[5] G. Sheng, S. Yang, J. Sheng, J. Hu, X. Tan, X. Wang, Macroscopic and microscopic investigation of Ni(II) sequestration on diatomite by batch, XPS, and EXAFS techniques, Environ. Sci. Technol. 45 (2011) 7718–7726.
[6] G. Sheng, L. Ye, Y. Li, H. Dong, H. Li, X. Gao, Y. Huang, EXAFS study of the interfacial interaction of nickel(II) on titanate nanotubes: Role of contact time, pH and humic substances, Chem. Eng. J. 248 (2014) 71–78.
[7] X.L. Tan, X.K. Wang, H. Geckeis, Th Rabung, Sorption of Eu(III) on humic acid or fulvic acid bound to alumina studied by SEM-EDS, XPS, TRLFS and batch techniques, Environ. Sci. Technol. 42 (2008) 6532–6537.
[8] G. Sheng, X. Shao, Y. Li, J. Li, H. Dong, W. Cheng, X. Gao, Y. Huang, Enhanced removal of U(VI) by nanoscale zerovalent iron supported on Na-bentonite and an investigation of mechanism, J. Phys. Chem. A 118 (2014) 2952–2958.
[9] D. Zhao, G. Sheng, J. Hu, C. Chen, X. Wang, The adsorption of Pb(II) on Mg_2Al layered double hydroxide, Chem. Eng. J. 171 (2011) 167–174.
[10] G. Sheng, Y. Li, H. Dong, D. Shao, Environmental condition effects on radionuclide 64Cu(II) sequestration to a novel composite: Polyaniline grafted multiwalled carbon nanotubes, J. Radioanal. Nucl. Chem. 293 (2012) 797–806.
[11] S. Yang, D. Zhao, H. Zhang, S. Lu, L. Chen, X. Yu, Impact of environmental conditions on the sorption behavior of Pb(II) in Na-bentonite suspensions, J. Hazard. Mater. 183 (2010) 632–640.
[12] G. Sheng, R. Shen, H. Dong, Y. Li, Colloidal diatomite, radionickel, and humic substance interaction: A combined batch, XPS, and EXAFS investigation, Environ. Sci. Pollut. Res. 20 (2013) 3708–3717.
[13] R. Hu, X. Wang, S. Dai, D. Shao, T. Hayat, A. Alsaedi, Application of graphitic carbon nitride for the removal of Pb(II) and aniline from aqueous solutions, Chem. Eng. J. 260 (2015) 469–477.
[14] S. Yang, C. Chen, Y. Chen, J. Li, D. Wang, X. Wang, W. Hu, Competitive adsorption of Pb(II), Ni(II) and Sr (II) ions on graphene oxides: A combined experimental and theoretical study, ChemPlusChem. 80 (2015) 480–484.
[15] G. Sheng, A. Alsaedi, W. Shammakh, S. Monaquel, J. Sheng, X. Wang, H. Li, Y. Huang, Enhanced sequestration of selenite in water by nanoscale zero valent iron immobilization on carbon nanotubes by a combined batch, XPS and XAFS investigation, Carbon 99 (2016) 123–130.
[16] S. Cataldo, A. Gianguzza, M. Merli, N. Muratore, D. Piazzese, M.L.T. Liveri, Experimental and robust modeling approach for lead(II) uptake by alginate gel beads: Influence of the ionic strength and medium composition, J. Colloid Interface Sci. 434 (2014) 77–88.
[17] G. Sheng, J. Hu, A. Alsaedi, W. Shammakh, S. Monaquel, F. Ye, H. Li, Y. Huang, A.S. Alshomrani, T. Hayat, B. Ahmad, Interaction of uranium(VI) with titanate nanotubes by macroscopic and spectroscopic investigation, J. Mol. Liq. 212 (2015) 563–568.
[18] G. Sheng, J. Hu, H. Li, J. Li, Y. Huang, Enhanced sequestration of Cr(VI) by nanoscale zero-valent iron supported on layered double hydroxide by batch and XAFS study. Chemosphere 148 (in press) 227–232.
[19] D. Xu, X. Tan, C. Chen, X. Wang, Removal of Pb(II) from aqueous solution by oxidized multiwalled carbon nanotubes, J. Hazard. Mater. 154 (2008) 407–416.
[20] D. Zhao, X. Yang, H. Zhang, C. Chen, Effect of environmental conditions on Pb(II) adsorption on β-MnO_2, Chem. Eng. J. 164 (2010) 49–55.
[21] G. Sheng, S. Wang, J. Hu, Y. Lu, J. Li, Y. Dong, X. Wang, Adsorption of Pb(II) on diatomite as affected via aqueous solution chemistry and temperature, Colloids Surf. A: Physicochem. Eng. Aspects 339 (2009) 159–166.
[22] J. Hu, D. Shao, C. Chen, G. Sheng, J. Li, X. Wang, M. Nagatsu, Plasma-induced grafting of cyclodextrin onto multiwall carbon nanotube/iron oxides for adsorbent application, J. Phys. Chem. B 114 (2010) 6779–6785.
[23] S. Yang, J. Hu, C. Chen, D. Shao, X. Wang, Mutual effects of Pb(II) and humic acid adsorptions on multiwalled carbon nanotubes/polyacrylamide composites from aqueous solutions, Environ. Sci. Technol. 45 (2011) 3621–3627.
[24] G. Sheng, Y. Li, X. Yang, X. Ren, S. Yang, J. Hu, X. Wang, Efficient removal of arsenate by versatile magnetic graphene oxide composites, RSC Adv. 2 (2012) 12400–12407.
[25] L. Peng, P. Qin, M. Lei, Q. Zeng, H. Song, J. Yang, J. Shao, B. Liao, J. Gu, Modifying Fe_3O_4 nanoparticles with humic acid for removal of Rhodamine B in water, J. Hazard. Mater. 209–210 (2012) 193–198.
[26] J.F. Liu, Z.S. Zhao, G.B. Jiang, Coating Fe_3O_4 magnetic nanoparticles with humic acid for high efficient removal of heavy metals in water, Environ. Sci. Technol. 42 (2008) 6949–6954.
[27] X. Zhang, Y. Wang, S. Yang, Simultaneous removal of Co(II) and 1-naphthol by core–shell structured Fe_3O_4@cyclodextrin magnetic nanoparticles, Carbohydr. Polym. 114 (2014) 521–529.
[28] S. Huang, D. Chen, Rapid removal of heavy metal cations and anions from aqueous solutions by an amino-functionalized magnetic nano-adsorbent, J. Hazard. Mater. 163 (2009) 174–179.
[29] Q. Fu, X. Zhou, L. Xu, B. Hu, Fulvic acid decorated Fe_3O_4 magnetic nanocomposites for the highly efficient sequestration of Ni(II) from an aqueous solution, J. Mol. Liq. 208 (2015) 92–98.
[30] T. Yamashita, P. Hayes, Analysis of XPS spectra of Fe^{2+} and Fe^{3+} ions in oxide materials, Appl. Surf. Sci. 254 (2008) 2441.
[31] Y. Li, G. Sheng, J. Sheng, Magnetite decorated graphene oxide for the highly efficient immobilization of Eu(III) from aqueous solution, J. Mol. Liq. 199 (2014) 474–480.
[32] G. Zhao, J. Li, X. Ren, C. Chen, X. Wang, Few-layered graphene oxide nanosheets as superior sorbents for heavy metal ion pollution management, Environ. Sci. Technol. 45 (2011) 10454–10462.

[33] K.F. Hayes, J.O. Leckie, Modeling ionic strength effects on cation adsorption at hydrous oxide/solution interfaces, J. Colloid Interface Sci. 115 (1987) 564–572.
[34] G. Sheng, H. Dong, Y. Li, Characterization of diatomite and its application for the retention of radiocobalt: Role of environmental parameters, J. Environ. Radioact. 113 (2012) 108–115.
[35] Q. Fan, D. Shao, Y. Lu, W. Wu, Effect of pH, ionic strength, temperature and humic substances on the sorption of Ni(II) to Na-attapulgite, Chem. Eng. J. 150 (2009) 188–195.
[36] G. Sheng, B. Hu, Role of solution chemistry on the trapping of radionuclide Th(IV) using titanate nanotubes as an efficient adsorbent, J. Radioanal. Nucl. Chem. 298 (2013) 455–464.
[37] C. Chen, X. Wang, Adsorption of Ni(II) from aqueous solution using oxidized multi-walled carbon nanotubes, Ind. Eng. Chem. Res. 45 (2006) 9144–9149.
[38] K.L. Mercer, J.E. Tobiason, Removal of arsenic from high ionic strength solutions: Effects of ionic strength, pH, and preformed versus in situ formed HFO, Environ. Sci. Technol. 42 (2008) 3797–3802.